Figure S1: RA enhances Treg cell conversion independently of nuclear RARα (Related to Figure 1)

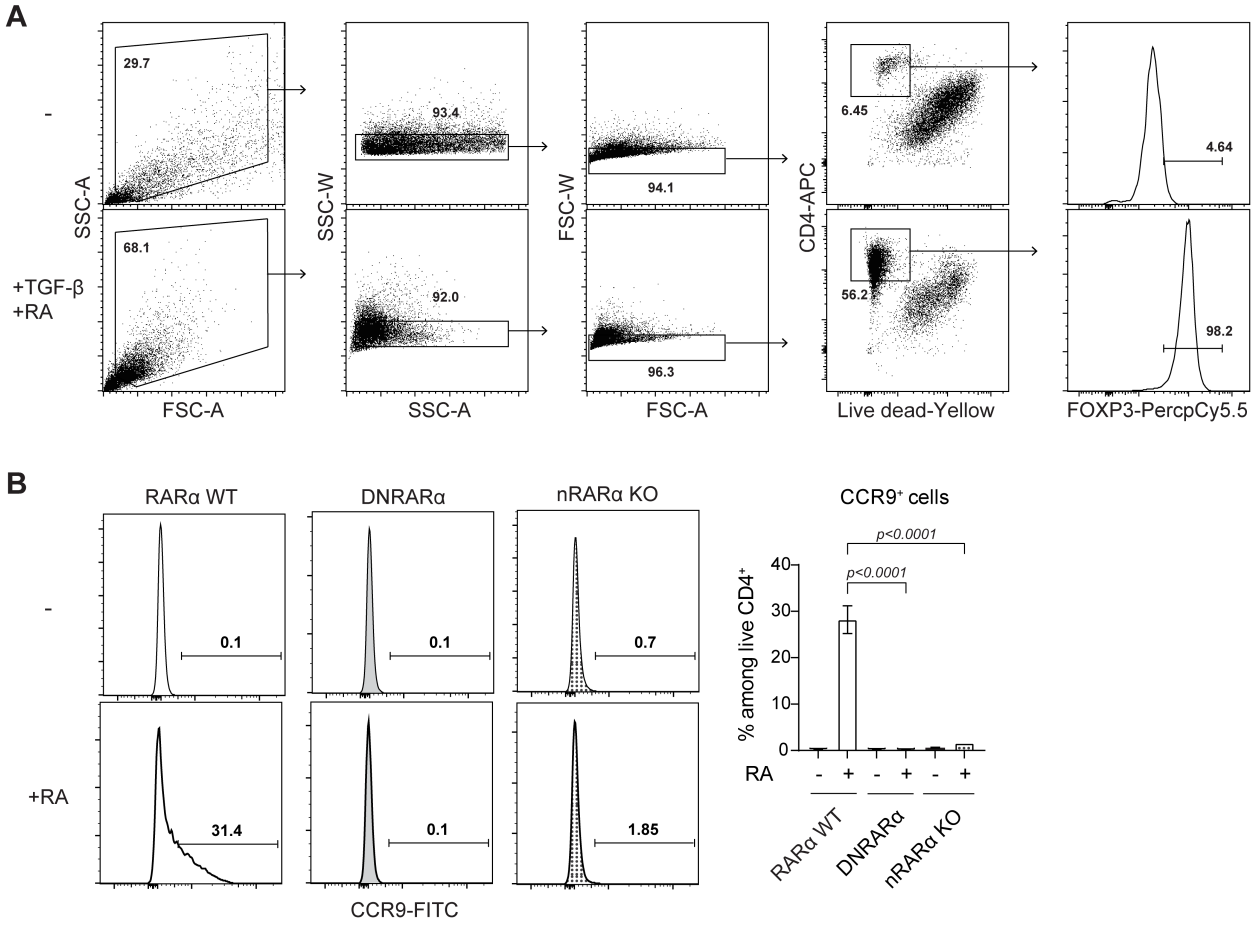

Figure S2: T cells express an extranuclear isoform of RARα (Related to Figure 2)

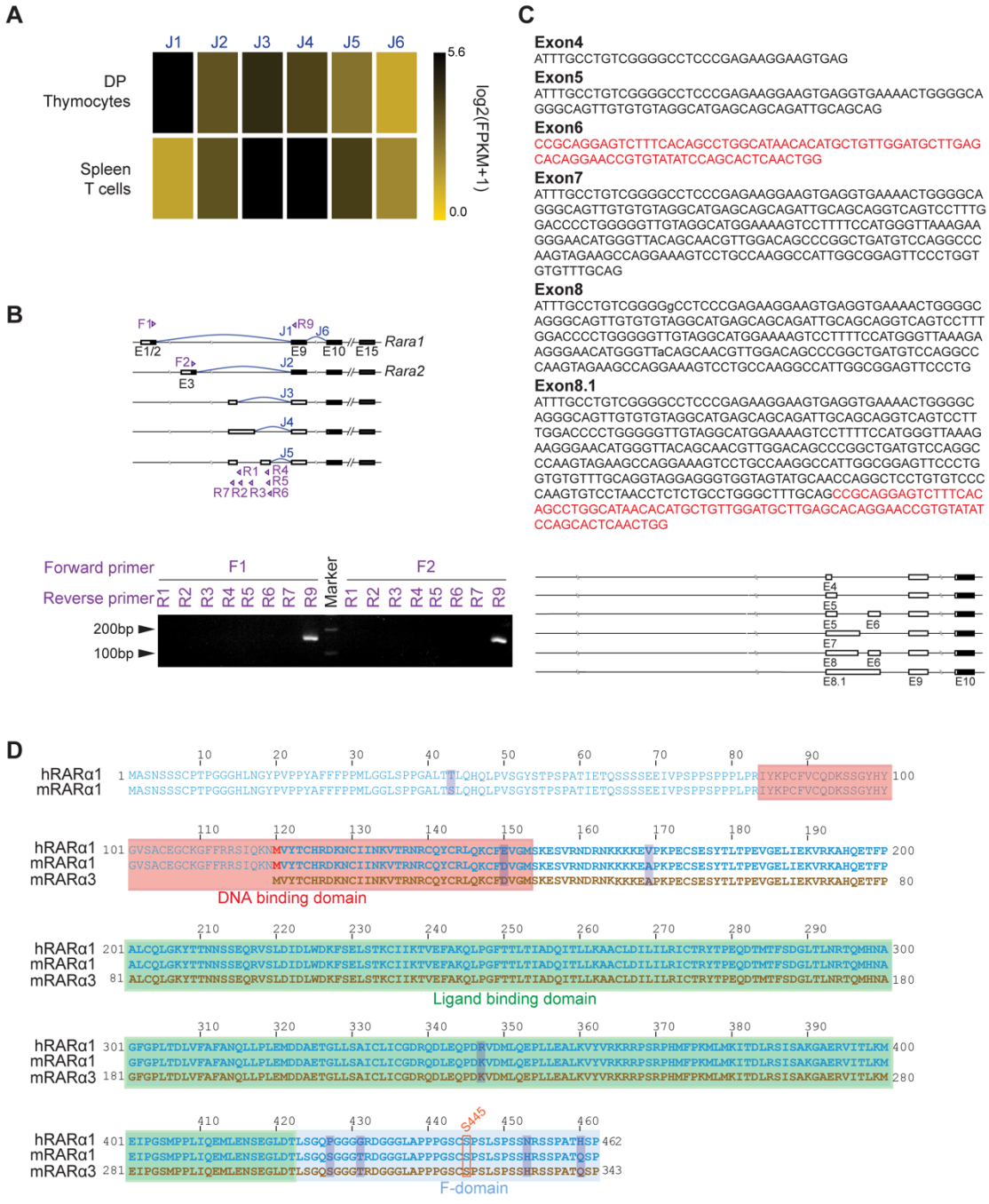

Figure S3: Extranuclear RARα controls TCR signal transduction (Related to Figure 3)

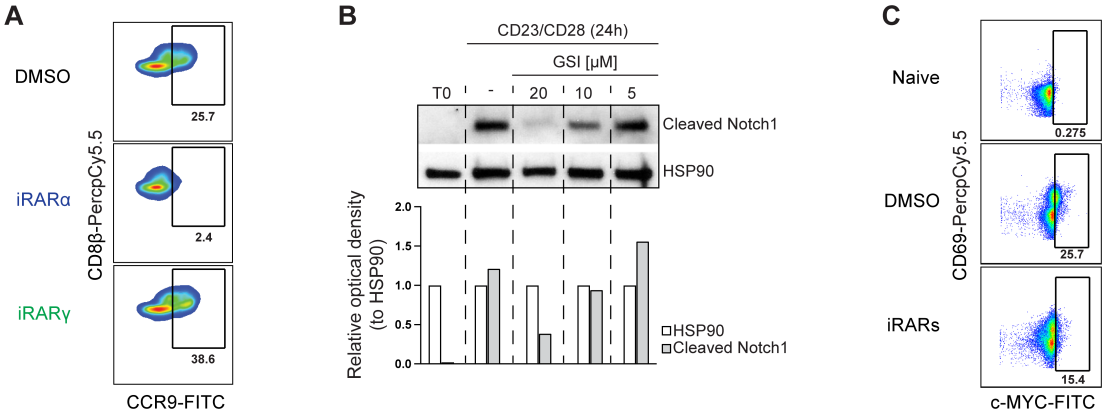

Figure S4: RA counteracts extranuclear RARα signaling in T cells (Related to Figure 5)

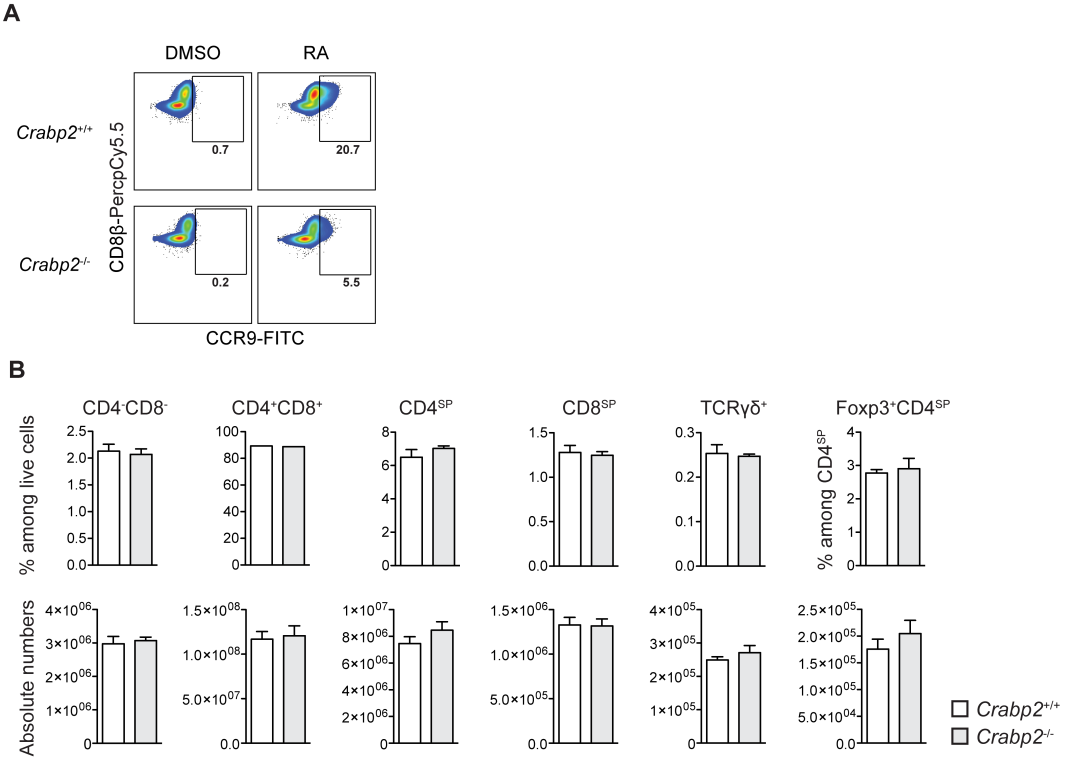

Figure S5: Extranuclear RARα signaling controls TCR-induced proliferation *in vivo* (Related to Figure 6)

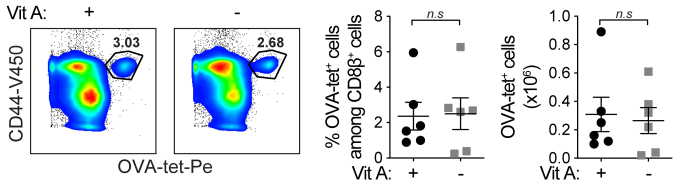

Figure S6: Extranuclear RARα signaling controls effector differentiation *in vivo* (Related to Figure 7)

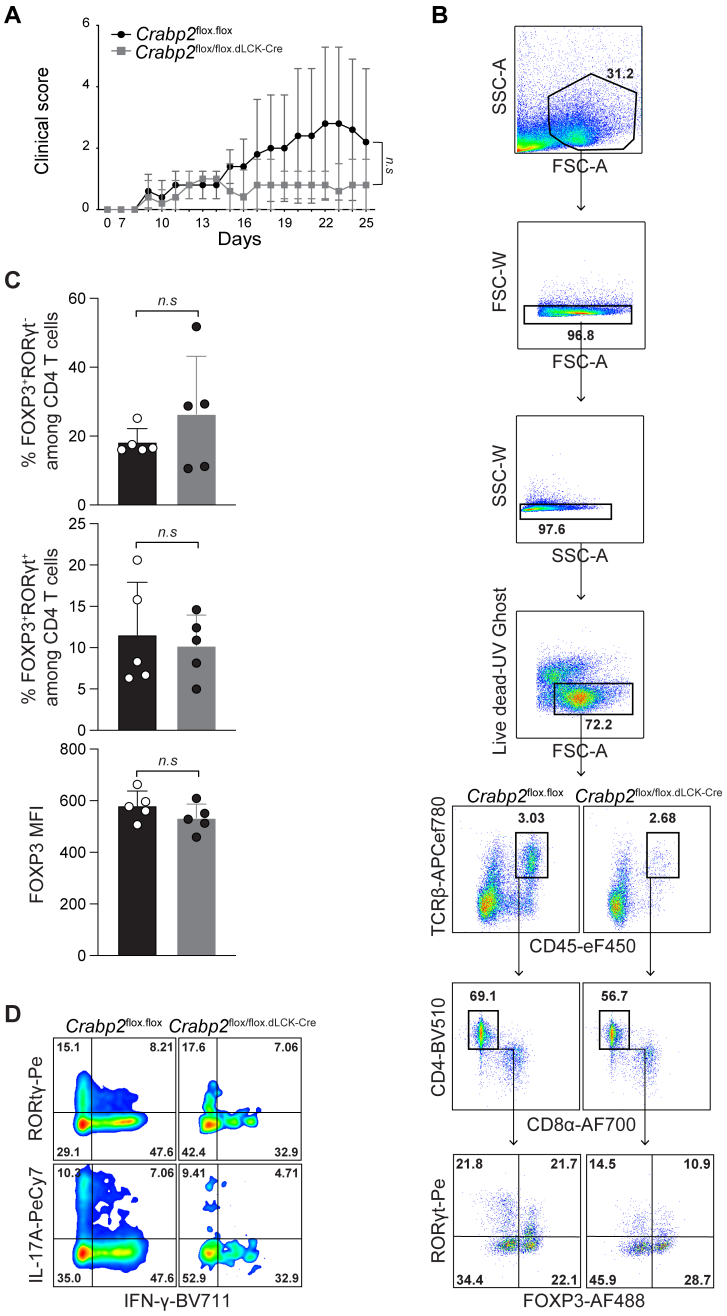

SUPPLEMENTAL FIGURE LEGENDS

FIGURE S1: RA enhances Treg cell conversion independently of nuclear RARα (Related to Figure 1)

(**A**) Gating strategy for analysis of FOXP3 expression among WT CD4 T cells stimulated for 96hrs with α-CD3/CD28 with or without TGF-β or RA. **(B)** Cell surface expression for CCR9 on WT, DNRARα or nRARα-deficient naïve spleen CD4 T cells stimulated for 16hrs *in vitro* with 1.0 μg/ml of plate-bound α-CD3 and 0.5 μg/ml of α-CD28, then cells were washed and cultured 48 more hours (64hrs in total) in cRPMI supplemented with 25 ng/ml of IL-2 with or without RA (10nM). Representative histograms of 2 independent experiments are shown. Statistical analyses of frequency of $CCR9^+$ T cells on the right was calculated with the two-tailed Student t-test. Mean +/- SEM is depicted.

FIGURE S2: T cells express an extranuclear isoform of RARα (Related to Figure 2)

(A) Heatmap for junction-use in spleen and DP thymocytes calculated and drawn by SG-seq package on R. **(B)** PCR analysis performed on cDNA from DP thymocytes using forward primers F1 and F2 in combination with reverse R primers as shown. F1+R9 and F2+R9 detect *Rara1* and *Rara2*, respectively. **(C)** DNA sequences of new exons as indicated. Shared sequence between exons 6 and 8.1 is in red. **(D)** Amino acid sequences of human and mouse RARα1 and mouse RARα3 are aligned. Lighter colored amino acids indicate mismatches between human and mouse. The first methionine used by mRARα3 is in red in the sequence of hRARα1 and mRARα1. The amino acid sequences shared by hRARα1 or mRARα1 and mRARα3 are in bold. Sequence encoding the DNA Binding

Domain (brown), the Ligand Binding Domain (green) and the F Domain (blue) are indicated. The numbers indicate amino acid number. Serine (S445) in the F Domain phosphorylated upon TCR stimulation is marked.

FIGURE S3: Extranuclear RARα controls TCR signal transduction (Related to Figure 3)

(**A**) Primary spleen T cells were treated with DMSO, a pan-RAR antagonist LE540 (iRARs), an RARα-specific antagonist, Ro 41-5253 (iRARα) or an RARγ antagonist, MM11253 (iRARγ) and activated with anti-CD3/CD28 in the presence of (10nM) RA for 72hrs. CCR9 expression was then assessed. Dot plots are from a representative experiment. Graphs represent the means +/- SEM of $CCR9^+$ T cells from 3 independent experiments. (**B**) Primary spleen T cells unstimulated or activated for 24hrs with anti-CD3/CD28 alone or with γ-secretase inhibitor (GSI) were analyzed with western blot for cleaved NOTCH1-intracellular domain with the quantification of its optical density relative to control HSP90. Representative western blot from 2 independent experiments. **(C)** Primary spleen T cells treated with DMSO or iRARs and activated with anti-CD3/CD28 for 4hrs were analyzed for the expression of c-MYC protein. Dot plots are from a representative experiment from three independent experiments.

FIGURE S4: RA counteracts extranuclear RARα signaling in T cells (Related to Figure 5)

(A) WT or CRABP2-deficient spleen T cells were activated with α-CD3/CD28 in the presence of RA (10nM) for 72hrs. CCR9 expression was then assessed. Dot plots show

one representative experiment out of three independent experiments. **(B)** Thymocytes isolated from 5 (10week-old and gender matched) WT and CRABP2-deficient mice were analyzed for phenotype, frequency and absolute number. Data are represented as the means +/- SEM.

FIGURE S5: Extranuclear RARα signaling controls TCR-induced proliferation *in vivo* (Related to Figure 6)

Tracking of endogenous OVA-reactive CD8 T cells in the spleen of WT $CD45.1^+CD45.2^+$ recipient mice with Vitamin A or Vitamin A-free, infected i.v. with $ActA^-$ Lm-OVA and assessed 7 days later. Graphs show the percentage and absolute number of OVA-reactive CD8 T cells among the total CD8 T cells.

FIGURE S6: Extranuclear RARα signaling controls effector differentiation *in vivo* (Related to Figure 7)

EAE was induced in WT and *Crabp2* conditional deletion mutant mice and cells from spinal cords were analyzed by FACs at day25 of EAE induction. (**A**) Clinical scores were assessed daily. (**B**) Gating strategy for live TCRβ and CD45 positive cells with a representative dot plot for FOXP3 and RORγt expressions. (**C**) Quantifications of $FOXP3^+ROR\gamma t^-$ Treg and $FOXP3^+ROR\gamma t^+$ cell frequencies and FOXP3 mean fluorescence intensity (MFI) among CD4 T cells. (**D**) Frequency of $IFN\gamma^+$ and $ROR\gamma t^+$ (upper) or $IL17A^+$(lower) cells are shown in representative dot plots. Data are representative of 2 independent EAE experiments. Statistical significance calculated with two-tailed Student t-test. Shown mean +/- SD.